Research Square

Preprints are preliminary reports that have not undergone peer review.
They should not be considered conclusive, used to inform clinical practice,
or referenced by the media as validated information.

Expanding the phenotype of EP300-related Rubinstein-Taybi syndrome: Evans syndrome and DNA methylation profiling in three individuals

Thibaut César

thibaut.cesar@aphp.fr

Université Paris Cité

Amandine Santini

Univ Rouen Normandie

Camille Charbonnier

Univ Rouen Normandie

Anne-Claire Richard

Univ Rouen Normandie

Gaël Nicolas

Univ Rouen Normandie

Anne Pagnier

Univ Grenoble Alpes

Nour El Housseini

Univ Grenoble Alpes

Eglantine Hullo

Univ Grenoble Alpes

Julien Thevenon

Univ Grenoble Alpes

Patricia Fergelot

Université de Bordeaux

Coralie Briand

Hôpital Jean-Verdier

Agathe Escudier

Centre Hospitalier Universitaire de Bordeaux

Bénédicte Neven

Université Paris Cité

Mony Fahd

Hôpital Robert-Debré

Sébastien Héritier

Hôpital Armand-Trousseau
Maria Merched
Centre Hospitalier Universitaire de Bordeaux
Didier Lacombe
Université de Bordeaux
Nathalie Aladjidi
Centre Hospitalier Universitaire de Bordeaux
Julien Gils
Université de Bordeaux

Research Article

Keywords: Chromatinopathies, Episignatures, Rubinstein-Taybi syndrome, Evans syndrome, Immune dysregulation, Syndromic primary immunodeficiency, Children

Posted Date: November 12th, 2026

DOI: https://doi.org/10.21203/rs.3.rs-11515893/v1

License: This work is licensed under a Creative Commons Attribution 4.0 International License.
Read Full License

Additional Declarations:
No competing interests reported.

Table 1 is available in the supplementary files section

Expanding the phenotype of *EP300*-related Rubinstein-Taybi syndrome: Evans syndrome and DNA methylation profiling in three individuals

Authors: Thibaut César[1*], Amandine Santini[2*], Camille Charbonnier[3], Anne-Claire Richard[2], Gaël Nicolas[2], Anne Pagnier[4], Nour El Housseini[4], Eglantine Hullo[4], Julien Thevenon[5], Patricia Fergelot[6], Coralie Briand[7], Agathe Escudier[8], Bénédicte Neven[1], Mony Fahd[9], Sébastien Héritier[10], Maria Merched[11], Didier Lacombe[6], Nathalie Aladjidi[8, 11*], Julien Van Gils[6*].

[1] Unité d'Immunologie, Hématologie et Rhumatologie Pédiatriques, AP-HP, Hôpital Necker-Enfants Malades, Université Paris Cité, Centre de Compétence CEREVANCE, Paris, France

[2] Université Rouen Normandie, Normandie Université, INSERM U1245 and CHU Rouen, Department of Genetics and Reference Center for Developmental Abnormalities, Rouen, France

[3] Department of Biostatistics and Reference Center for Developmental Abnormalities, Université Rouen Normandie, Normandie Université, INSERM U1245 and CHU Rouen, Rouen, France

[4] Département de Pédiatrie, CHU Grenoble Alpes, Université Grenoble Alpes, Centre de Compétence CEREVANCE, Grenoble, France.

[5] Service de Génétique, CHU Grenoble Alpes, Université Grenoble Alpes, Grenoble, France.

[6] Service de Génétique Médicale, CHU de Bordeaux, INSERM U1211 MRGM, Université de Bordeaux, Bordeaux, France.

[7] Département de Pédiatrie, AP-HP, Hopital Jean Verdier, Centre de Compétence CEREVANCE, Bondy, France.

[8] Service d'hémato-immunologie pédiatrique, CIC1401, INSERM CIC-P, CHU de Bordeaux, Bordeaux, France.

[9] Unité d'Hématologie Pédiatrique, AP-HP, Hôpital Robert Debré; Centre de Référence National des Cytopénies Autoimmunes de l'Enfant (CEREVANCE), Paris, France.

[10] Unité d'Hématologie Pédiatrique, AP-HP, Hôpital Trousseau; Centre de Référence National des Cytopénies Autoimmunes de l'Enfant (CEREVANCE), Paris, France.

[11] Centre de Référence National des Cytopénies Auto-immunes de l'Enfant (CEREVANCE), CHU de Bordeaux, Bordeaux, France

[*] Contributed equally

Corresponding author: Thibaut César

Unité d'Immunologie, Hématologie et Rhumatologie Pédiatriques

Hôpital Necker, 149 rue de Sèvres, 75015 Paris, France.

Email: thibaut.cesar@aphp.fr

Abstract

Background: Rubinstein-Taybi syndrome type 2 (RTS2) is a rare chromatinopathy caused by pathogenic variants in *EP300* and is characterised by developmental delay, distinctive facial dysmorphic features, and broad extremities. Chromatinopathies are increasingly recognised as syndromic primary immune deficiency and dysregulation (PIDD) disorders associated with autoimmune complications, but the full immunological spectrum of RTS2 remains incompletely understood. The French OBS'CEREVANCE cohort has included all consecutive cases of paediatric-onset autoimmune cytopenia from participating centres since 2004 and provides prospective, long-term observational follow-up. Leveraging this unbiased national database, which includes 406 patients with paediatric-onset Evans syndrome (pES) with a median follow-up of 9 years, we identified three children with pES and RTS2.

Results: All patients exhibited typical clinical features of RTS2 and carried heterozygous pathogenic variants in *EP300* (two *de novo* stop-gain variants, c.1942C>T and c.4933C>T, and one missense variant in the catalytic domain, c.4351C>T). Severe autoimmune cytopenias were diagnosed at 4, 5, and 7 years of age and required prolonged immunomodulatory therapies. Two patients had non-malignant lymphoproliferation, including one with granulomatous-lymphocytic interstitial lung disease. Immunological evaluations revealed variable humoral and cellular abnormalities, including hypogammaglobulinemia; deficiencies in naïve CD4 T cells, naïve CD8 T cells, and switched memory B cells; and a positive interferon signature. Comprehensive genetic investigations excluded alternative monogenic causes of PIDD. Genome-wide DNA methylation profiling demonstrated that all three patients with pES clustered with reference *EP300* pathogenic variant carriers, confirming the presence of the robust *EP300* episignature, without a distinct secondary DNA methylation signature specifically differentiating the pES phenotype. Longitudinal blood samples showed stable epigenetic profiles over time.

Conclusions: This study expands the phenotypic spectrum of *EP300*-related RTS by identifying pES as a severe manifestation of immune dysregulation associated with this chromatinopathy. Although these patients display the canonical *EP300* DNA methylation episignature, the absence of a distinct secondary methylation profile suggests complex, multifactorial contributions to autoimmunity. Clinicians should be aware of this rare association, to ensure prompt immunological evaluation and follow-up in patients with *EP300*-related RTS and prompt genetic evaluation of paediatric or adult patients with ES by haemato-immunologists.

Keywords

Chromatinopathies, Episignatures, Rubinstein-Taybi syndrome, Evans syndrome, Immune dysregulation, Syndromic primary immunodeficiency, Children

Background

Evans syndrome (ES) is defined by the simultaneous or sequential occurrence of two or three autoimmune cytopenias (AICs), including immune thrombocytopenia (ITP), autoimmune haemolytic anaemia (AIHA), and autoimmune neutropenia. ES represents a severe form of immune dysregulation and is increasingly recognised as a clinical indicator of an underlying primary immune deficiency and dysregulation (PIDD), particularly in children. In paediatric populations, AIHA and ITP occur far more

frequently in patients with PIDD than in the general population, with an estimated risk at least 120-fold higher (1). Accordingly, current recommendations emphasise the need to investigate potential monogenic causes of paediatric Evans syndrome (pES), with a causative molecular diagnosis established in up to 40% of cases (2). Identifying such genetic etiologies is critical, as it may refine prognosis, guide immunological monitoring, and inform targeted therapeutic strategies.

Rubinstein-Taybi syndrome (RTS) is a rare developmental disorder caused by pathogenic variants in *CREBBP* (RTS type 1, OMIM #180849; 80–85% of cases) or *EP300* (RTS type 2, OMIM #613684; 15–20% of cases). It is characterised by distinctive craniofacial features, broad thumbs and halluces, intellectual disability, and postnatal growth deficiency. These genes encode transcriptional coactivators with intrinsic histone acetyltransferase activity that regulate gene expression through histone acetylation and chromatin remodelling (3). RTS is inherited in an autosomal dominant manner but occurs sporadically in most patients, with an estimated incidence of 1 in 100,000 to 1 in 125,000 births (4). Although RTS type 2 was initially considered to have a milder phenotype, more recent data suggest that it is better characterised as phenotypically variable, with substantial clinical overlap with RTS type 1 (5).

CREBBP and *EP300* belong to a growing group of genes implicated in chromatinopathies, a class of congenital disorders resulting from disturbances in chromatin regulation and epigenetic balance (6). These conditions share overlapping clinical features and are associated with disorder-specific DNA methylation (DNAm) profiles, known as episignatures (7–9). Episignatures have emerged as valuable diagnostic biomarkers for chromatinopathies, enabling the classification of molecular subtypes and improving variant interpretation. Beyond their diagnostic utility, they also provide insights into disease mechanisms and may contribute to the development of targeted therapeutic strategies aimed at correcting disease-specific epigenetic dysregulation (10–12).

Several chromatinopathies have recently been recognised as syndromic forms of PIDD associated with immune defects and dysregulation. Kabuki syndrome, caused by pathogenic variants in *KMT2D* or

KDM6A, demonstrates this overlap between epigenetic regulation and immune homeostasis. Patients with Kabuki syndrome frequently exhibit immune dysfunction, including recurrent infections, hypogammaglobulinemia, and autoimmune manifestations. AICs represent the most common autoimmune complications of this condition (13). In contrast, the immunological phenotype of RTS remains less well-characterised. In a cohort of 97 adults and children with RTS, infections were reported in 72% and autoimmune manifestations in 12.3%, including AICs in 6.2% of patients; notably, no cases of ES were described (14). To date, a single case of pES associated with RTS in a 14-year-old patient has been reported (15,16). Current international recommendations for RTS management highlight the risk of recurrent infections and recommend immunological evaluation when clinically indicated, particularly to assess for hypogammaglobulinemia; however, they do not specifically address the potential risk of autoimmune complications (17).

Leveraging the French OBS'CEREVANCE cohort of paediatric-onset AIC, we report three cases of pES associated with Rubinstein-Taybi syndrome type 2 (RTS2), further supporting a link between chromatinopathies and immune dysregulation.

These observations raise the possibility that immune dysregulation in RTS, particularly in association with *EP300* variants, may be underrecognised. Expanding the clinical spectrum of immune manifestations in RTS could facilitate the early recognition of immune complications and inform patient management.

Methods

Patient selection

Since 2004, following appropriate consent, patients with chronic ITP, AIHA, or ES diagnosed before 18 years of age have been included in the French national OBS'CEREVANCE cohort (30 French centres), which provides prospective observational follow-up (NCT05937828). Immunogenetic studies using next-generation sequencing panels, trio whole-exome sequencing (WES), or trio whole-genome sequencing (WGS) are offered to patients with pES (ACTION trial, ANR-18-CE17-0001, NCT03912129,

2019–2023) and have been extended to patients with isolated ITP or AIHA associated with immunopathological manifestations.

We screened the OBS'CEREVANCE cohort to identify patients reported as having RTS as a comorbidity of AIC.

Data were extracted from the observational OBS'CEREVANCE database on June 1, 2025. When necessary, medical records and follow-up data were updated in collaboration with each participating centre. Photographs were collected when available to review the patients' morphological characteristics and confirm that they fulfilled the clinical diagnostic criteria for RTS (17).

Episignature profiling is routinely performed in France for patients with chromatinopathies. The results for these patients were also collected.

This study was approved by the Ethics Committee of Bordeaux University Hospital (CER-BDX 2025-293), and a specific informed consent form for the publication of data and photographs was signed by the patients' legal representatives.

DNAm profiling

Genomic DNA was extracted from whole blood and subjected to bisulphite conversion. DNAm profiles were quantified using Infinium MethylationEPIC v2.0 BeadChips (Illumina, 20087708), in accordance with the manufacturer's protocol. Samples from the three patients with ES carrying an *EP300* variant (including, for two patients, a second sample collected at a younger age) were processed together with a reference cohort of *EP300* pathogenic variant carriers (n = 15) and healthy controls (n = 118), balanced across 95 arrays and array rows to reduce technical biases. All methylation arrays were processed similarly at the ASGARD-Rouen genomic platform (University of Rouen and Rouen University Hospital) and scanned using the same Illumina NextSeq 550 scanner.

DNAm analysis

Raw Illumina intensity data files were processed and normalised using the default Meffil package protocol together with all other samples included in the 95 arrays to estimate more accurately the variability of methylation signals within and across arrays. Several predictions were derived from methylation values, to apply standard quality-control and normalisation procedures. All samples of interest (ES patients and positive and negative controls) met the quality-control requirements. Sex predictions were extracted from the standard Meffil normalised object. Blood cell counts were estimated using the 'meffil.cell.count.estimates' function, and DNAm age was predicted using the 'DNAmAge' function of the methylclock package. These estimates were consistent with the age at sampling and reported sex for all samples. Because ES affects the immune system, particular attention was paid to differences in the estimated blood cell distributions among groups. Samples were functionally normalised together, as recommended in the Meffil documentation, with random-effect adjustment for array and Sentrix row and fixed-effect adjustment for the first two principal components, before computing β values. Specifically, for each probe, a baseline methylation-level model adjusted for skinHorvath age at sampling, sex, and blood cell composition was fitted using negative-control samples. Adjusted methylation levels were then calculated for each sample as the difference between the normalised β values and the expected baseline levels for the sample's age at sampling, sex, and blood cell composition.

Identification and exclusion of age-associated probes

As several patients were sampled during early childhood, and because blood DNAm is known to vary significantly with age during the first years of life, we sought to identify and exclude probes whose methylation levels were primarily driven by age rather than *EP300* disease status. This approach was used to prevent the disease-specific signature from being confounded by age-related methylation drift. To this end, two complementary approaches were applied independently within *EP300* pathogenic variant carriers and healthy controls. First, probe-wise Pearson correlation tests between normalised methylation values and age at sampling were performed across the genome. Probes reaching a

nominal *p*-value below 1×10^{-7} were classified as age-correlated. Second, to account for potential nonlinear newborn-specific effects, samples were divided into two age groups (< 1 year vs. ≥ 1 year), and two-sample *t*-tests were performed for each probe between the two groups. Probes with a nominal p-value below 1×10^{-7} were classified as age-discriminant. The union of all probes identified by either method (correlation or age-stratum comparison), in either the *EP300* pathogenic group or the control group, was defined as the set of age-associated probes. This combined set of age-associated probes was excluded from the normalised methylation matrix before all downstream analyses, including the epigenome-wide association studies (EWAS) used to derive the *EP300* disease signature described below. This strategy minimised the risk of age-driven methylation variation being misattributed to the *EP300*-associated episignature.

Episignature detection and validation

The *EP300*-associated DNAm signature was established through an EWAS ('meffil.ewas' function) comparing healthy controls with *EP300* pathogenic variant carriers. The analysis was adjusted for skinHorvath clock, sex, and estimated blood cell composition. A stringent combination of *p*-value < 1×10^{-7} and $|\Delta\beta| > 0.1$ was used to select differentially methylated positions, which were retained as the final signature for downstream analyses.

The overall structure of the dataset was summarised using principal component analysis (PCA) restricted to the signature probes. Unsupervised hierarchical clustering was performed using Euclidean distance and Ward's aggregation method, and the results were visualised as a heatmap using the pheatmap package. Phenotypic status was annotated as control, *EP300* pathogenic variant carrier, or *EP300* pathogenic variant carrier with ES. The probes were partitioned into two blocks by cutting the hierarchical tree ('cutree', k = 2), and the average methylation level per block was compared between groups using Wilcoxon tests (raincloud plots).

To evaluate predictive performance, a support vector machine (SVM) model with a linear kernel was implemented using the e1071 package, with probability estimation enabled. To investigate the classification of patients with ES relative to other samples while ensuring the independence of observations and preventing overfitting, ES patients were systematically excluded from model training and reserved exclusively for downstream testing and visualisation. SVM analyses used a binary classification contrasting negative controls with *EP300* individuals. To enable a fair comparison with predictions for ES patients, SVM scores for positive controls were also computed using 5-fold cross-validation to reduce overfitting. Following model training, predicted probabilities were extracted for visualisation. Training *EP300* sample scores represent SVM scores for positive controls when all positive controls were included in the training set. Validation scores represent SVM scores for positive controls when they were included in the validation set of the 5-fold cross-validation framework.

A second, independent EWAS was conducted to specifically investigate whether the co-occurrence of ES was associated with a distinct methylation signature within *EP300* pathogenic variant carriers, rather than with the presence or absence of the *EP300* signature relative to controls. This EWAS directly contrasted *EP300* pathogenic variant carriers without ES (grouped with controls as the reference category, 'EP300_Control') with *EP300* pathogenic variant carriers with ES ('EP300_Evans'). The same covariate adjustment strategy (DNAm age, sex, and blood cell composition) and *p*-value/effect-size thresholds were applied to derive candidate probes specific to the Evans-associated phenotype. The same analyses and visualisations were performed (PCA, heatmap, raincloud plots, and SVM). However, to evaluate predictive performance, a leave-one-out scheme was used, in which one ES patient was excluded when training the model.

A PCA restricted to the previously published RTS2 (*EP300*) episignature probes (9) was also performed on all samples.

All statistical analyses of DNAm profiles were performed using R (version 4.1.2).

Results

As of June 1, 2025, 2,334 patients were included in the OBS'CEREVANCE cohort, including 406 with pES, with a median follow-up of 9 years (0.1–42.9). Among these patients, three from three distinct centres were identified as having sequential or simultaneous ES and RTS. All three carried a variant in *EP300*. The diagnosis of RTS type 2 was reviewed and confirmed based on molecular and clinical expertise. Additionally, no patient with a pathogenic *CREBBP* or *EP300* variant was identified by WES in the ACTION trial, and no patient with isolated ITP or AIHA had an RTS phenotype reported in the OBS'CEREVANCE database.

P1, a male, was born prematurely and eutrophic to non-consanguineous Algerian parents, with no information available regarding possible preeclampsia. Congenital athyreosis was diagnosed following standard neonatal screening. Micropenis and cryptorchidism were also noted. Dysmorphic features included pes planus, hypertrichosis, and facial and dental abnormalities (Figure 1A). The subsequent course was characterised by neurodevelopmental delay, delayed acquisition of walking, and persistent primary enuresis. Moderate asthma was reported from 1.5 to 5 years of age.

After his arrival in France at the age of 10 years, neurodevelopmental assessment revealed microcephaly (48 cm, −3 SD) and an intelligence quotient of 66. Brain and spinal MRI findings were normal. Next-generation sequencing targeting causes of microcephaly identified a *de novo* pathogenic variant in the *EP300* gene (NM_001429.4: c.1942C>T; p.Arg648Ter; ACMG: PVS1, PS2; ClinVar-NCBI Variation ID: 6882).

ITP occurred at the age of 7 years and was treated with corticosteroids (CS). A relapse occurred 2 months later, requiring a further 1.5 months of CS therapy. At the age of 9 years, he developed warm AIHA, which was treated with CS (2 mg/kg/day), tapered over 4 months, followed by a relapse 5 months later. CS were reintroduced (2 mg/kg/day), with additional high-dose CS boluses (15 mg/kg/day from D9 to D11) for refractory AIHA. CS were tapered from day 30 and discontinued after 5 months. He was 15 years old at the last follow-up, with no further ITP or AIHA relapse.

Immunological work-up (Table 2) revealed hypogammaglobulinemia associated with recurrent pneumonia and bronchiectasis, negative post-immunisation serologies, low switched memory B-cell levels, elevated autoreactive B-cell levels, low naïve CD4 and CD8 T-cell levels, and a positive interferon signature. WES performed in the ACTION trial revealed no additional pathogenic variant involved in PIDD. Non-malignant hepatomegaly and splenomegaly gradually developed. Immunoglobulin replacement therapy was initiated at the age of 13 years, resulting in clinical improvement.

P2, a male, was born at term to non-consanguineous Moroccan parents with a prenatally diagnosed complex congenital heart disease, including transposition of the great arteries, ventricular septal defect, atrial septal defect, and a cleft mitral valve. He presented with microcephaly, congenital hip dislocation, and hypoparathyroidism associated with dysmorphic facial features (Figure 1B). Cardiac surgery was performed during the neonatal period and was associated with subtotal thymectomy. He developed severe, fixed non-convulsive encephalopathy (non-communicative patient), with severe oral disorders and skeletal abnormalities (scoliosis). Brain MRI showed vermian hypotrophy and a significantly enlarged cistern.

A missense variant in *EP300* (NM_001429.4: c.4351C>T; p.(His1451Tyr); ACMG: PM1, PM2, PP3, PP5; likely pathogenic; ClinVar-NCBI Variation ID: 4056384) was identified in the histone acetyltransferase domain following exome sequencing for neurodevelopmental delay.

At the age of 4 years, 1 week after a mild episode of gastroenteritis, he developed warm AIHA. He responded well to CS at 2 mg/kg/day, achieving a complete response at 4 weeks, which allowed CS tapering. Seven months after AIHA onset, he presented with a haemorrhagic syndrome with a Buchanan-Adix score of 3, leading to a diagnosis of severe ITP. No infectious trigger was identified. Anti-platelet antibodies were positive. The disease course was complex, with severe cutaneomucosal haemorrhages despite intravenous immunoglobulin and CS therapy, ultimately requiring rituximab and romiplostim to achieve platelet remission. A transient relapse occurred 1 year after rituximab,

when B cells reappeared, and a second course was administered. He was 6 years old at the last follow-up and was receiving daily antibiotic prophylaxis.

Immunological investigations revealed no significant quantitative B- or T-cell abnormalities, and the interferon signature was positive. WGS revealed no pathogenic variant suggestive of IEI. Pulmonary investigations led to the diagnosis of asymptomatic granulomatous lymphocytic interstitial lung disease (GLILD), which was managed with continuous antibiotic prophylaxis; no additional immunosuppressive treatment was administered.

P3 was a male born prematurely and hypotrophic to non-consanguineous parents by caesarean section because of maternal acute pulmonary oedema and preeclampsia. He presented with microcephaly and multiple malformations, including a double aortic arch causing tracheomalacia and oesophageal compression (surgically corrected at the age of 3 months), a spontaneously closed interventricular communication, incomplete abnormal pulmonary venous return, cryptorchidism, enlarged thumbs, and facial dysmorphism (Figure 1C). He subsequently exhibited moderate developmental delay, requiring special-needs schooling. He had moderate asthma and eosinophilic esophagitis in a familial atopic context.

In this context, exome sequencing revealed a pathogenic *de novo* variant in the *EP300* gene (NM_001429.4: c.4933C>T; p.Arg1645*, also designated p.Arg1645Ter; ACMG: PVS1, PS2; ClinVar-NCBI Variation ID: 183678), with no other pathogenic immunological variant identified.

At the age of 5 years, he presented with simultaneous ES, comprising ITP with a Buchanan-Adix score of 3, neutropenia, and moderate signs of AIHA, with a haemoglobin level of 9.8 g/dL, haemolysis, and a positive Coombs test for IgG and C3d. A context of multiple infections was identified as a potential trigger, with positive nasal PCR tests for rhinovirus and adenovirus, as well as primary *Cytomegalovirus* infection. Complete remission was achieved with intravenous immunoglobulin administered every 2 weeks for 3 months and CS at 2 mg/kg/day, tapered and discontinued over 1.5 months. He was 7 years old at the last follow-up.

Immunological investigations revealed normal immunoglobulin levels, lymphocyte phenotyping, and proliferation testing. Antinuclear antibodies with anti-SSA specificity and anti-thyroperoxidase antibodies were detected. No additional immunopathological manifestations were observed.

DNAm profile of ES patients along the *EP300* episignature

Given the particular autoimmune profile of patients with ES, we first confirmed the absence of altered blood cell composition, as estimated by DNAm. Estimated blood cell composition showed no significant differences between controls, *EP300* pathogenic variant carriers, and ES patients across the six examined cell populations (granulocytes, monocytes, NK cells, B cells, CD4+ T cells, and CD8+ T cells), confirming the absence of a major cell-composition confounder in the methylation analysis (Supplementary Figure 1).

Before establishing our own episignature, we assessed whether the previously published RTS2 episignature (9) could be directly applied to our cohort. Projection onto this probe set showed less clear separation between *EP300* pathogenic variant carriers and controls (PC1, 29.6% of variance explained) than that subsequently achieved with our newly derived signature (PC1, 38.7%). An apparent age-related drift was also observed between longitudinal samples from the same patient (P2/P2_young and P3/P3_young), motivating the identification and exclusion of age-associated probes and the derivation of a cohort-specific signature (Supplementary Figure 2).

Genome-wide epigenetic association analysis comparing 15 typical *EP300* patients with 118 healthy controls led to the identification of 321 differentially methylated CpG positions. PCA restricted to these *EP300* signature probes revealed clear separation between controls and pathogenic variant carriers along the first axis (38.7% of variance explained), whereas the second axis accounted for only 6.6% of the variance. All five samples from the three ES patients (P1, P2, P2_young, P3, and P3_young) projected within the cluster of reference *EP300* pathogenic variant carriers, confirming that they displayed the expected typical *EP300* episignature. Age at sampling had no effect on the location of duplicate samples along the first principle component. The ES patient with the most attenuated

episignature intensity (P2, positioned closest to the control cluster on PC1) carried a missense *EP300* variant, in contrast to the stop-gain variants identified in the other two ES patients (P1 and P3), which were associated with a stronger episignature. Similarly, among the reference *EP300* pathogenic variant carriers, the two individuals positioned closest to the control cluster carried a missense and a splice-site variant, respectively, whereas carriers of frameshift variants tended to display a stronger episignature (Figure 2A).

Unsupervised hierarchical clustering confirmed this separation into two main clusters, with ES samples clustering with *EP300* pathogenic variant carriers rather than with negative controls (Figure 2C). This analysis identified two distinct blocks, one hypomethylated and the other hypermethylated. We focused on these two homogeneous blocks of probes by examining the density distributions of the average methylation levels within each block across all individuals (Figure 2D, E). The within-block distributions revealed significant methylation differences between controls and *EP300* pathogenic variant carriers and between controls and ES patients, with no significant difference between *EP300* pathogenic variant carriers and ES patients, confirming comparable signature intensity between the latter two groups.

As expected, near-perfect specificity and sensitivity were achieved in the training set, reflecting the complete separation between the controls and *EP300* pathogenic variant carriers used to construct the signature. In the 5-fold cross-validation setting, which assessed the internal reproducibility of the episignature, sensitivity exceeded 0.75 (95% binomial exact confidence interval, CI [0.595; 0.983]) for all validation samples except the two samples carrying a missense and a splice-site variant, respectively, consistent with the attenuated episignature intensity observed for these variants on PCA. For the ES patients, predictions obtained either from the full training set or from the corresponding cross-validation training blocks yielded highly consistent results. Patients P1 and P3 showed a very high probability of pathogenicity, confirming that they shared the *EP300* episignature, whereas patient P2

again displayed an intermediate probability, of the same order of magnitude as that of the two reference *EP300* carriers with attenuated signatures described above (Figure 2B).

Search for an Evans-specific methylation signature within *EP300* carriers

To determine whether ES is associated with a specific methylation signature distinct from the *EP300* episignature, we performed a dedicated EWAS directly comparing *EP300* pathogenic variant carriers without ES (combined with controls as the reference group) with *EP300* pathogenic variant carriers with ES. Preliminary inspection of this analysis suggested that, unlike the robust and highly significant *EP300*-vs.-control signature, the direct comparison of *EP300* carriers with and without ES yielded a considerably smaller set of differentially methylated positions (n = 58).

PCA restricted to these differentially methylated positions revealed marked heterogeneity among the three ES patients. Two patients (P2 and P3, including their respective younger timepoints) clustered together and separated from both negative controls and *EP300* pathogenic variant carriers, whereas P1 clustered closely with the negative controls and *EP300* pathogenic variant carrier group. The first two principal components explained 38.2% and 9.8% of the variance, respectively (Figure 3A).

Consistently, unsupervised hierarchical clustering visualised on the heatmap showed that P2 and P3 clustered together and separated from a second cluster comprising P1, negative controls, and *EP300* pathogenic variant carriers. Two probe blocks were identified, one hypomethylated and the other hypermethylated. However, within the P2/P3 cluster, several probes displayed heterogeneous methylation intensities, indicating limited robustness of this candidate episignature across biological duplicates (Figure 3C). Raincloud plots further illustrated this heterogeneity. For the hypomethylated block, P2 and P3 showed an approximately 25% difference in methylation relative to negative controls and *EP300* pathogenic variant carriers, whereas the difference was only approximately 15% for P1. For the hypermethylated block, methylation differences ranged from approximately 5% for P1 to nearly 30% for P2_young, further underscoring the lack of a homogeneous methylation pattern across the three ES patients (Figure 3D, E).

When the SVM classifier trained on the full dataset was used to predict the probability of carrying both an *EP300* variant and ES, negative controls and *EP300* pathogenic variant carriers showed probabilities close to 0, as expected, whereas ES patients showed sensitivity close to 100%, except for P1, whose probability was comparatively lower, consistent with the attenuated signal observed in the preceding analyses. To further assess whether ES patients shared a common, reproducible methylation episignature, we performed a leave-one-out analysis in which all duplicates of each ES patient were sequentially excluded, a new candidate signature was derived from the remaining two patients, and the excluded patient was then independently tested using the corresponding SVM model. In each iteration, the model failed to accurately predict the excluded patient (Figure 3B).

Discussion

We report a series of three cases presenting the rarely described association between pES and RTS due to *EP300* mutations, together with their epigenetic signatures.

All patients fulfilled the recognised clinical diagnostic criteria for RTS (17). They also illustrated phenotypic characteristics distinguishing *EP300*-related RTS from *CREBBP*-related RTS. Preeclampsia, experienced by P2's mother, has been reported in 23–33% of pregnancies involving children with *EP300* variants, compared with approximately 3% in patients with *CREBBP* variants and in the general population (5). All three children had microcephaly, which has been reported in 82% and 53% of patients with *EP300* and *CREBBP* mutations, respectively (5). The dysmorphic features observed here were classically milder, as reported in the *EP300* cohort (18), and were dominated by hypertrichosis, a low posterior hairline, arched eyebrows, long eyelashes, micrognathia, dental abnormalities, foetal fingertip pads, and broad halluces. Similarly, neurocognitive impairment is usually moderate in patients with *EP300* variants. P2 represents an exception, with unusually severe neurocognitive disability that initially cast doubt on the diagnosis. However, the absence of another genetic abnormality on WGS and the compatibility of the remainder of the clinical phenotype supported the diagnosis of RTS.

All *EP300* mutations identified in the patients reported here were *de novo*, and two resulted in a premature stop codon (P1 and P3), making their pathogenicity indisputable. P2 carried a missense variant in the acetylation domain, which is part of the catalytic domain that is functionally crucial for the protein and in which all but three of the reported *EP300* point mutations are located (5). *EP300* is a gene in which polymorphisms are frequently identified and is associated with a broader phenotypic spectrum than *CREBBP*. Furthermore, among patients with the rare RTS (1/125,000), *EP300* mutations are considerably less frequent than *CREBBP* mutations (8–11% vs. 55–75% of the cases), making it likely that additional aspects of the clinical phenotype remain to be described.

The three patients reported here presented with a combination of at least two AICs during childhood, occurring at the ages of 7, 4, and 5 years in P1, P2, and P3, respectively. These cytopenias occurred simultaneously in P3 and sequentially in P1 and P2. This finding supports the implementation of specialised follow-up with a complete work-up after a first immunological event, to allow appropriate adaptation of long-term preventive measures. P1 and P3 had a relatively straightforward course, with a complete response to first-line treatment. P2 required a combination of second-line treatments with rituximab and romiplostim. The occurrence of ES in children is a strong marker of immune dysregulation; a causative genetic defect associated with IEI is identified in 40% of pES cases and strongly suspected in an additional 25% of cases (2).

To our knowledge, only one other case of pES associated with RTS has been reported, also involving a patient carrying an *EP300* missense variant (c.4767T>C; p.Met1588Thr) (15,16). The addition of three patients with this extremely rare combination is therefore noteworthy. The immunological phenotype of patients with RTS was investigated in detail in a retrospective multicentre cohort of 97 paediatric and adult patients (14). Only 50.5% of patients had an established molecular diagnosis, including 44 with *CREBBP* and five with *EP300* variants. No genotype-phenotype correlation could be established, and a key finding was that a second genetic anomaly potentially responsible for IEI should be ruled out, as one patient was ultimately found to carry a variant in the *MEFV* gene and two patients carried

the common monoallelic *BAFF-R* polymorphism (c.62C>G; p.Pro21Arg). All patients reported here underwent extensive genetic analyses, with particular attention to genes involved in PIDD (WES, n = 2; WGS, n = 1), and no causative immunological defect other than *EP300* was identified.

The immunopathological manifestations reported in RTS are highly variable. In the cohort reported by Saettini et al. (14), infections were highly prevalent, occurring in 72% of patients, with respiratory infections reported in 55% of cases; 22% experienced severe infections requiring hospitalisation. Manifestations of immune dysregulation were reported in 12.3% of patients, including six cases of AIC affecting only one cell line, although the molecular diagnoses in these cases were not specified. Non-malignant lymphoproliferation was present in 8.2% of patients and included lymphadenopathy, hepatomegaly, and/or splenomegaly. Immunological laboratory investigations revealed hypo-IgG and hypo-IgM in 12.7% and 18.2% of patients, respectively. The most notable abnormalities on lymphocyte phenotyping were naïve CD4 T-cell lymphopenia in four of 10 patients (40%), B-cell lymphopenia in 22.7%, and decreased switched memory B cells in five of 13 patients (38.5%). Ten patients (16.4%) received immunoglobulin replacement therapy, with clinical benefit. These findings are consistent with our observations. Only P1 had hypogammaglobulinemia, accompanied by reduced naïve CD4 and CD8 T cells and switched memory B cells, recurrent lower respiratory tract infections, and clinical benefit following the initiation of immunoglobulin replacement therapy. Non-malignant lymphoproliferative manifestations were present in P1 and P2, with hepatosplenomegaly in P1 and a clinical presentation of GLILD in P2, without respiratory consequences to date. To our knowledge, the latter manifestation has not previously been described in RTS. P1 and P2 had increased autoreactive B cells and a positive interferon signature. The interferon signature was negative in P3, but was measured 1 year after his episode of pES. These observations involve too few patients to draw robust conclusions regarding the inflammatory pathways implicated in this context.

It is important to note a potential confounding factor regarding the autoimmunity observed in P2, as he underwent subtotal thymectomy during the neonatal period, which may have contributed to both

autoimmunity and immune deficiency. This factor may be underreported in patients with congenital heart disease in RTS cohorts.

Our study demonstrated that patients with ES carrying pathogenic *EP300* variants exhibit the newly identified DNAm episignature associated with RTS2. Despite presenting an unusual autoimmune phenotype extending beyond the classical clinical spectrum of RTS2, all three patients were consistently classified within the *EP300* molecular group by unsupervised analyses and machine-learning approaches. These findings indicate that the presence of ES neither weakens nor modifies the constitutive *EP300* episignature, supporting the robustness of this molecular biomarker across a broader phenotypic spectrum than previously described. Of note, the p.(His1451Tyr) variant in the histone acetyltransferase domain clustered with loss-of-function truncating variants, confirming, through this common episignature, the deleterious consequences of this missense variant.

To determine whether the occurrence of ES is associated with additional constitutional methylation changes beyond the *EP300* episignature, we performed a dedicated EWAS comparing *EP300* pathogenic variant carriers with and without ES. In contrast to the robust and reproducible methylation signature distinguishing *EP300* patients from controls, this analysis identified only a limited number of differentially methylated positions, which failed to define a consistent methylation profile across the three ES patients. Unsupervised analyses revealed substantial interindividual heterogeneity, and leave-one-out validation demonstrated that candidate episignatures derived from two patients were unable to accurately classify the third. Collectively, these findings do not support the existence of a common and reproducible constitutional DNAm signature specifically associated with ES in *EP300*-related disease.

Several explanations may account for this negative finding. First, the rarity of ES among individuals with pathogenic *EP300* variants limited the statistical power of our study. Although repeated sampling increased the number of samples analysed, the number of independent patients remained very small, making the identification of subtle methylation differences particularly challenging. Second, ES itself is

clinically and biologically heterogeneous and involves multiple immune pathways that may differ among patients despite similar clinical manifestations. Such heterogeneity could obscure a common epigenetic signal. Nevertheless, our study cannot exclude the presence of discrete and strong patient-specific epimutations.

Interestingly, longitudinal samples obtained from two patients demonstrated remarkable stability of their methylation profiles over time. Despite being collected during early childhood, a developmental period characterised by substantial physiological changes in methylation, paired samples remained closely associated on PCA and yielded comparable SVM classification scores. This observation further supports the temporal stability of the *EP300* episignature and reinforces its value as a diagnostic biomarker throughout childhood. More broadly, the comparable estimated blood cell composition among groups, together with the systematic exclusion of age-associated CpG sites before signature derivation, strengthens confidence that the observed methylation differences primarily reflect the constitutional consequences of *EP300* dysfunction rather than confounding related to age or cell composition.

Conclusions

The combination of pES and RTS associated with an *EP300* mutation is extremely rare and highlights the value of close collaboration among specialists in both clinical care and medical research.

For geneticists following patients with *EP300* mutations, it appears appropriate to educate parents and first-line caregivers to recognise clinical signs of cytopenia (haemorrhagic syndrome, jaundice, pallor, and recurrent infections) and to perform a complete blood count with reticulocyte count and blood smear at least once a year. Associated manifestations of immune dysregulation should also prompt immunological investigations.

For immunohaematologists caring for paediatric or adult patients, it appears worthwhile to refer patients with AIC associated with dysmorphic features or a neurodevelopmental disorder for clinical

genetics consultation, particularly because the clinical phenotype associated with *EP300* mutations can be subtle in this regard.

Our preliminary findings suggest a potential novel epigenetic pathophysiological component of autoimmunity and warrant further investigation to identify potential targeted therapeutic strategies.

List of Abbreviations

AIC: autoimmune cytopenia

AIHA: autoimmune haemolytic anaemia

CS: corticosteroids

ES: Evans syndrome

EWAS: epigenome-wide association studies

GLILD: granulomatous lymphocytic interstitial lung disease

IEI: inborn error of immunity

ITP: immune thrombocytopenia

IVIg: intravenous immunoglobulins

PCA: principal component analysis

pES: paediatric Evans syndrome

RTS: Rubinstein-Taybi syndrome

SVM: support vector machine

WES: whole exome sequencing

WGS: whole genome sequencing

Declarations

Ethics approval and consent to participate

This study was conducted in accordance with the principles of the Declaration of Helsinki. Approval was granted by the Research Ethics Committee of Centre Hospitalier Universitaire de Bordeaux (CER-BDX 2025-293).

Consent for publication

Informed consent was obtained from all individual participants included in the study or from their parents or legal guardians.

Availability of data and materials

All clinical data generated or analysed during this study are included in this published article and its supplementary information files. Methylation data generated at the Rouen ASGARD platform have been deposited in the European Genome-phenome Archive (EGA), hosted by EMBL-EBI, under study accession number EGAS00001008070 (https://ega-archive.org/studies/EGAS00001008070).

Competing interests

The authors declare that they have no competing interests.

Funding

The CEREVANCE network has been supported since 2001 by the AFSE, ARMHE, and O'CYTO patient associations; since 2007 by Bordeaux University Hospital and the French Ministry of Health (Rare Disease Plans 2007, 2017, and 2023); and since 2014 by the French Filière Maladies Rares Immuno-Hématologiques (MARIH). Genetic immunological studies were supported by the Institut National de la Santé et de la Recherche Médicale (INSERM) and by government grants managed by the Agence Nationale de la Recherche as part of the "Investment for the Future" programme (Institut Hospitalo-Universitaire Imagine, grant ANR-18-CE17-0001 "ACTION"); by Inserm as part of the 2022 MESSIDORE

program (project Inserm-MESSIDORE 19) to CC. AS received grants from Région Normandie and GIRCI Nord Ouest (FHU-A2M2P).

Authors' contributions

TC, NA, and JVG designed the study. TC, NA, MM, and JVG collected the clinical data. AS and CC generated the episignature data. TC, AS, CC, NA, and JVG analysed the data. TC, AP, NEH, EH, JT, PF, CB, AE, BN, DL, NA, and JVG provided clinical care to the patients. TC, AS, CC, NA, and JVG wrote the manuscript, which was reviewed, edited, and approved by all co-authors.

Acknowledgements

We thank the families for their participation and for sharing relevant information. We also thank the MaRIH and Handirare rare disease networks for fostering an environment conducive to these collaborations.

References

1. Fischer A, Provot J, Jais JP, Alcais A, Mahlaoui N, Adoue D, et al. Autoimmune and inflammatory manifestations occur frequently in patients with primary immunodeficiencies. J Allergy Clin Immunol. 1 nov 2017;140(5):1388-1393.e8. doi:10.1016/j.jaci.2016.12.978

2. Hadjadj J, Aladjidi N, Fernandes H, Leverger G, Magérus-Chatinet A, Mazerolles F, et al. Pediatric Evans syndrome is associated with a high frequency of potentially damaging variants in immune genes. Blood. 4 juill 2019;134(1):9-21. doi:10.1182/blood-2018-11-887141

3. Roelfsema JH, White SJ, Ariyürek Y, Bartholdi D, Niedrist D, Papadia F, et al. Genetic Heterogeneity in Rubinstein-Taybi Syndrome: Mutations in Both the CBP and EP300 Genes Cause Disease. Am J Hum Genet. avr 2005;76(4):572-80. doi:10.1086/429130 PubMed PMID: 15706485; PubMed Central PMCID: PMC1199295.

4. Hennekam RCM. Rubinstein–Taybi syndrome. Eur J Hum Genet. sept 2006;14(9):981-5. doi:10.1038/sj.ejhg.5201594

5. Van Gils J, Magdinier F, Fergelot P, Lacombe D. Rubinstein-Taybi Syndrome: A Model of Epigenetic Disorder. Genes. 24 juin 2021;12(7):968. doi:10.3390/genes12070968 PubMed PMID: 34202860; PubMed Central PMCID: PMC8303114.

6. Bjornsson HT. The Mendelian disorders of the epigenetic machinery. Genome Res. oct 2015;25(10):1473-81. doi:10.1101/gr.190629.115 PubMed PMID: 26430157; PubMed Central PMCID: PMC4579332.

7. Sadikovic B, Levy MA, Aref-Eshghi E. Functional annotation of genomic variation: DNA methylation episignatures in neurodevelopmental Mendelian disorders. Hum Mol Genet. 15 sept 2020;29(R1):R27-32. doi:10.1093/hmg/ddaa144

8. Beck DB, Petracovici A, He C, Moore HW, Louie RJ, Ansar M, et al. Delineation of a Human Mendelian Disorder of the DNA Demethylation Machinery: TET3 Deficiency. Am J Hum Genet. 6 févr 2020;106(2):234-45. doi:10.1016/j.ajhg.2019.12.007 PubMed PMID: 31928709; PubMed Central PMCID: PMC7010978.

9. Levy MA, McConkey H, Kerkhof J, Barat-Houari M, Bargiacchi S, Biamino E, et al. Novel diagnostic DNA methylation episignatures expand and refine the epigenetic landscapes of Mendelian disorders. Hum Genet Genomics Adv. 3 déc 2021;3(1):100075. doi:10.1016/j.xhgg.2021.100075 PubMed PMID: 35047860; PubMed Central PMCID: PMC8756545.

10. Nava AA, Arboleda VA. The omics era: a nexus of untapped potential for Mendelian chromatinopathies. Hum Genet. 2024;143(4):475-95. doi:10.1007/s00439-023-02560-2 PubMed PMID: 37115317; PubMed Central PMCID: PMC11078811.

11. Vos N, Reilly J, Elting MW, Campeau PM, Coman D, Stark Z, et al. Dna Methylation Episignatures are Sensitive and Specific Biomarkers for Detection of Patients with Kat6A/Kat6B Variants. Epigenomics. 1 mars 2023;15(6):351-67. doi:10.2217/epi-2023-0079 PubMed PMID: 37249002.

12. Kerkhof J, Squeo GM, McConkey H, Levy MA, Piemontese MR, Castori M, et al. DNA methylation episignature testing improves molecular diagnosis of Mendelian chromatinopathies. Genet Med. 1 janv 2022;24(1):51-60. doi:10.1016/j.gim.2021.08.007

13. Margot H, Boursier G, Duflos C, Sanchez E, Amiel J, Andrau JC, et al. Immunopathological manifestations in Kabuki syndrome: a registry study of 177 individuals. Genet Med. 1 janv 2020;22(1):181-8. doi:10.1038/s41436-019-0623-x

14. Saettini F, Herriot R, Prada E, Nizon M, Zama D, Marzollo A, et al. Prevalence of Immunological Defects in a Cohort of 97 Rubinstein–Taybi Syndrome Patients. J Clin Immunol. 1 août 2020;40(6):851-60. doi:10.1007/s10875-020-00808-4

15. Saettini F, Moratto D, Grioni A, Maitz S, Iascone M, Rizzari C, et al. A novel EP300 mutation associated with Rubinstein-Taybi syndrome type 2 presenting as combined immunodeficiency. Pediatr Allergy Immunol. 2018;29(7):776-81. doi:10.1111/pai.12968

16. Saettini F, Fazio G, Bonati MT, Moratto D, Massa V, Di Fede E, et al. Identical EP300 variant leading to Rubinstein–Taybi syndrome with different clinical and immunologic phenotype. Am J Med Genet A. 2022;188(7):2129-34. doi:10.1002/ajmg.a.62719

17. Lacombe D, Bloch-Zupan A, Bredrup C, Cooper EB, Houge SD, García-Miñaúr S, et al. Diagnosis and management in Rubinstein-Taybi syndrome: first international consensus statement. J Med Genet. juin 2024;61(6):503-19. doi:10.1136/jmg-2023-109438 PubMed PMID: 38471765; PubMed Central PMCID: PMC11137475.

18. Fergelot P, Van Belzen M, Van Gils J, Afenjar A, Armour CM, Arveiler B, et al. Phenotype and genotype in 52 patients with Rubinstein–Taybi syndrome caused by EP300 mutations. Am J Med Genet A. 2016;170(12):3069-82. doi:10.1002/ajmg.a.37940



Figure 1. Morphological characteristics of patients with *EP300* mutations.

Photographs of (A) P1, (B) P2, and (C) P3 at 2 years of age. The patients notably share microcephaly, hypertrichosis, a low posterior hairline, arched eyebrows, long eyelashes, micrognathia, dental abnormalities, foetal fingertip pads, and broad halluces. (D) Summary of the morphological characteristics of the patients.

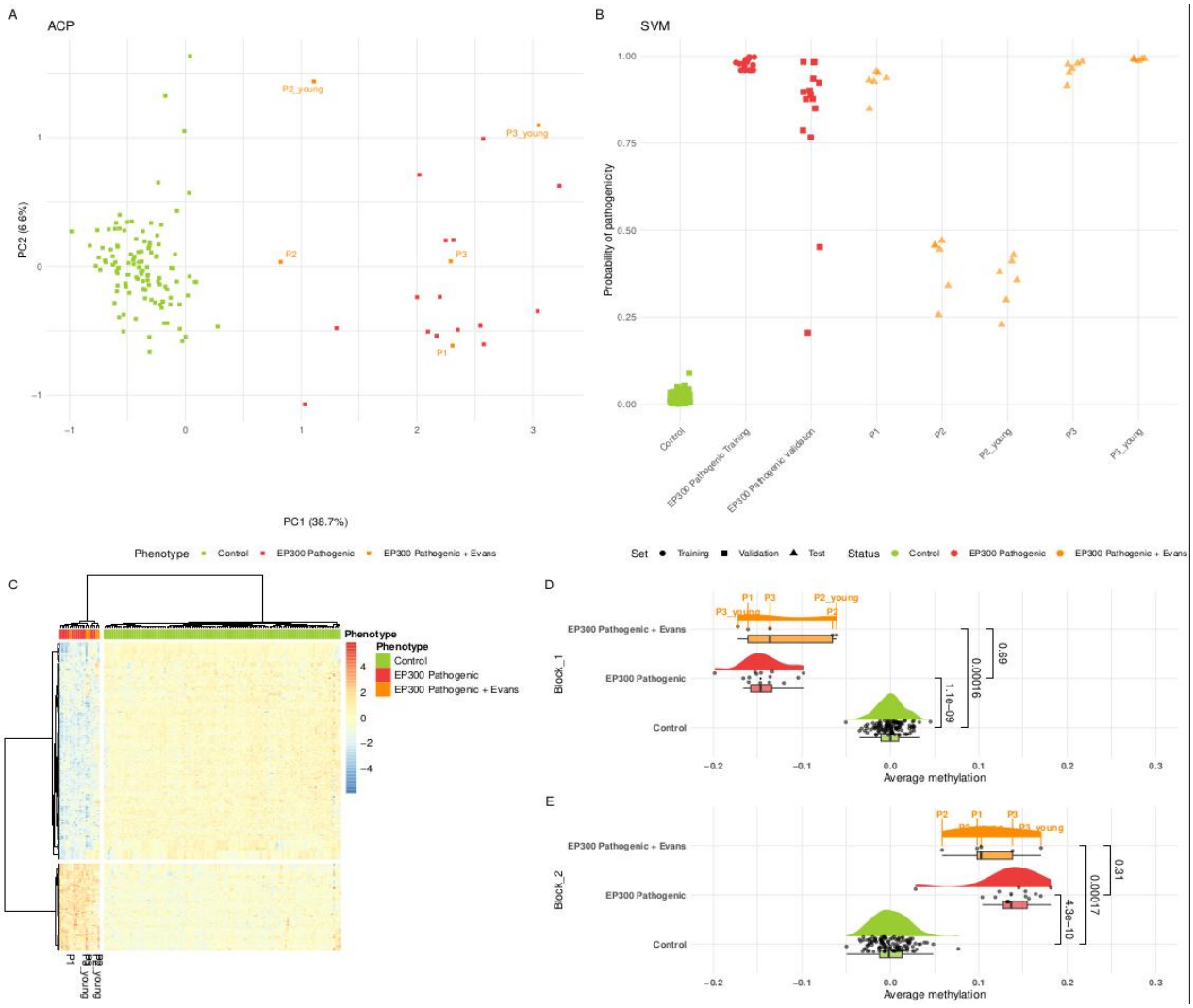


Figure 2. Patients with Evans syndrome carrying pathogenic *EP300* variants display the *EP300* DNA methylation episignature.

(A) Principal component analysis performed using the *EP300* DNA methylation signature derived from the EWAS comparing healthy controls with *EP300* pathogenic variant carriers. Evans syndrome patients (P1, P2, and P3, including longitudinal samples from P2 and P3) cluster with reference *EP300* pathogenic variant carriers and separate from healthy controls. Percentages indicate the proportion of variance explained by each principal component. Control: green; *EP300* pathogenic: red; *EP300* pathogenic + Evans: orange.

(B) Support vector machine classification scores. Positive controls were evaluated using a five-fold cross-validation framework, whereas Evans syndrome patients were excluded from model training and classified as independent test samples. Each point represents the predicted probability of carrying an *EP300* pathogenic variant.

(C) Unsupervised hierarchical clustering performed using the *EP300* signature probes. Rows represent CpG probes, and columns represent individual samples.

(D) Average methylation levels of probe block 1, as identified in panel C. Each point represents one sample. Horizontal bars indicate group medians. *P*-values were calculated using Wilcoxon rank-sum tests.

(E) Average methylation levels of probe block 2, as identified in panel C. Each point represents one sample. Horizontal bars indicate group medians. P values were calculated using Wilcoxon rank-sum tests.

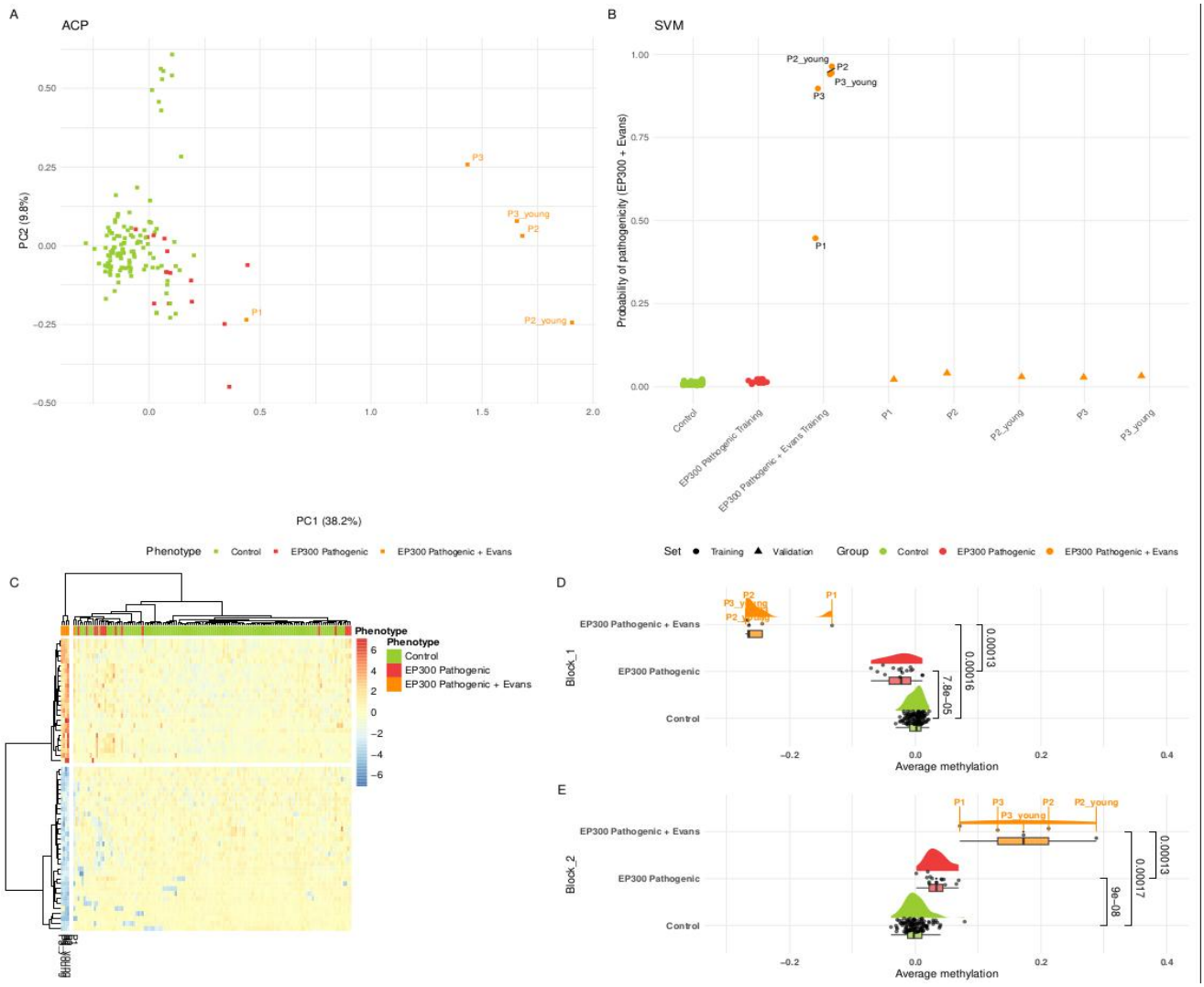


Figure 3. Identification of candidate DNA methylation changes associated with Evans syndrome in *EP300* pathogenic variant carriers.

(A) Principal component analysis performed using candidate probes identified by the EWAS comparing *EP300* pathogenic variant carriers with Evans syndrome with the reference group comprising healthy controls and *EP300* pathogenic variant carriers without Evans syndrome. Percentages indicate the proportion of variance explained by each principal component. Control: green; *EP300* pathogenic: red; *EP300* pathogenic + Evans: orange.

(B) Support vector machine classification scores obtained using the Evans syndrome candidate signature. Evans syndrome patients were evaluated using a leave-one-out strategy, in which each patient was sequentially excluded from signature derivation and independently classified. Each point represents the predicted probability of belonging to the *EP300* + Evans group.

(C) Unsupervised hierarchical clustering based on the candidate Evans syndrome-associated probes. Rows represent CpG probes, and columns represent individual samples.

(D) Average methylation levels of probe block 1, as identified in panel C. Each point represents one sample. Horizontal bars indicate group medians. *P*-values were calculated using Wilcoxon rank-sum tests.

(E) Average methylation levels of probe block 2, as identified in panel C. Each point represents one sample. Horizontal bars indicate group medians. *P*-values were calculated using Wilcoxon rank-sum tests.

Table 1. Clinical and molecular characteristics of the patients (cf. Excel).

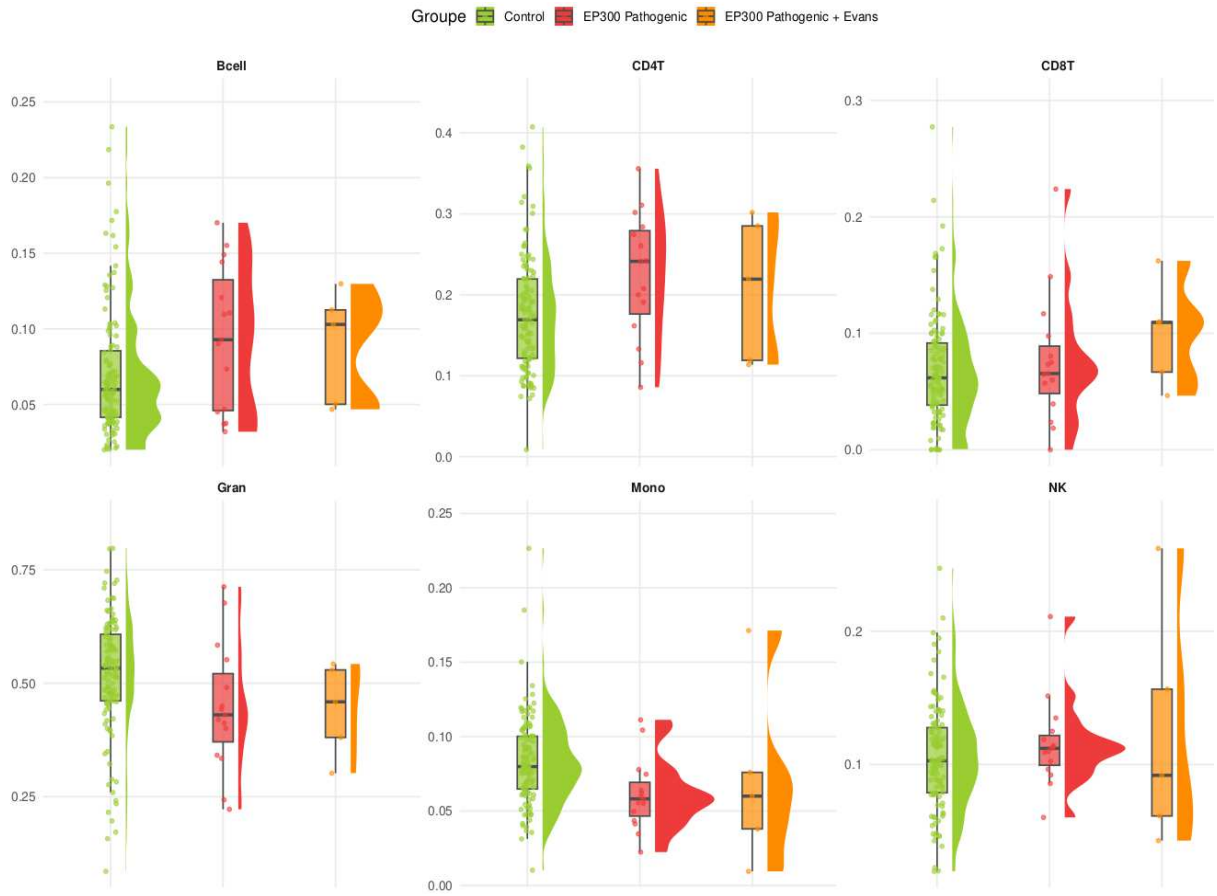
673 **Table 2. Immunological work-up performed outside treatment periods in three patients with pES**
674 **and RTS due to *EP300* mutations.**

675 Laboratory reference ranges are provided in parentheses. ANA, antinuclear antibody; IFN, interferon.

	P1 (10 y)	P2 (4 y)	P3 (7 y)
IgG (g/L)	3.8 (7.6–15.5)	7.74 (5.4–18.2)	8.5 (5.5–10.2)
IgA (g/L)	0.29 (0.6–3.5)	0.36 (0.21–2.91)	1.14 (0.46–1.5)
IgM (g/L)	0.74 (0.35–2.4)	2.08 (0.41–2.4)	1.98 (0.54–2.4)
Post-vaccination serologies	Tetanus negative *Pneumococcus* negative	Tetanus positive Diphtheria positive	Tetanus negative *Pneumococcus* positive
Lymphocytes (/µL)	5380 (1900–3700)	4861 (2300–5400)	2900 (1900–3700)
T-cells (/µL)	4508 (1200–2600)	3330 (1400–3700)	2120 (1200–2600)
CD4 T-cells (/µL)	3518 (650–1500)	1600 (700–2200)	1130 (650–1500)
naive CD4 T-cells (%)	15 (43–55)	45 (46–72)	58 (32–68)
CD8 T cells (/µL)	914 (370–1100)	1290 (490–1300)	870 (370–1100)
naive CD8 CCR7+CD45RA+ (%)	40 (52–68)	27 (29–72)	32 (30–61)
centr mem CCR7+CD45RA-/CD8 (%)	2.2 (3–4)	10 (2–13)	0 (2–12)
eff mem CCR7-CD45RA-/CD8 (%)	35.2 (11–20)	16 (14–49)	3 (20–45)
TEMRA CCR7-CD45RA+ (%)	22.7 (16–28)	47 (5–25)	65 (7–26)
Double negative T cells	N	N	N
B cells (/µL)	763 (2019–509)	747 (390–1400)	360 (270–860)
naive B cells IgD+CD27- (%)	77.5 (59–85)	71 (76.3–84.9)	80.3 (59.7–88.4)
marginal zone B cells IgD+CD27+ (%)	19.6 (3–21)	18.7 (4–9)	10.3 (3.1–18)
switched memory B cells IgD-CD27+ (%)	2.1 (4.4–20.5)	5.3 (3.3–7.4)	7.2 (2.9–17.4)
Transitional B cells CD24+CD38+ (%)	4.5 (3.9–7.8)	0.75 (5.4–9.2)	17.8
auto-reactive B cells CD21-CD38- (%)	6.2 (0.9–3.3)	19.5 (1.8–5.2)	NA
NK cells (/µL)	552 (130–720)	772 (130–720)	230 (100–480)
IFN signature	5.6 (<2)	4 (<2.3)	Negative
ANA	Negative	1/160	1/160, Anti-SSA 20 UI/L

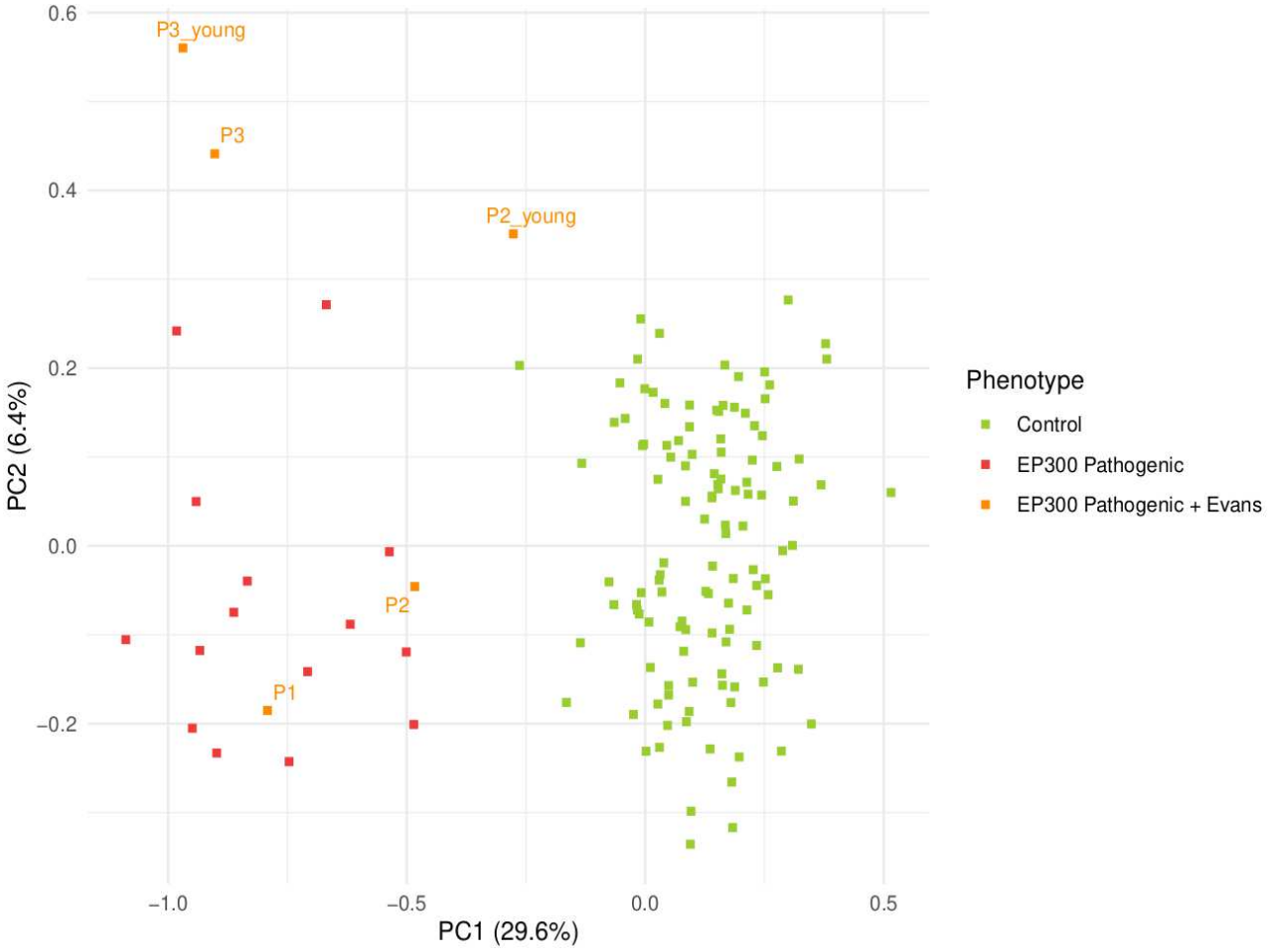
676

677 Additional Material



678

679 **Supplementary Figure 1. Estimated blood cell composition in healthy controls, *EP300* pathogenic**
680 **variant carriers, and *EP300* pathogenic variant carriers with Evans syndrome.** Estimated proportions
681 of granulocytes (Gran), monocytes (Mono), natural killer cells (NK), B cells (Bcell), CD4+ T cells (CD4T),
682 and CD8+ T cells (CD8T) were inferred from DNA methylation data using the Meffil cell-count
683 estimation algorithm. Each point represents one sample, and horizontal bars indicate group medians.



Supplementary Figure 2. Projection of study samples onto the previously published RTS2 (*EP300*) DNA methylation signature. Principal component analysis restricted to CpG probes from the previously reported RTS2 episignature (Levy et al., 2021). Percentages indicate the proportion of variance explained by each principal component. Control: green; *EP300* pathogenic: red; *EP300* pathogenic + Evans: orange. Evans syndrome samples (P1, P2, P2_young, P3, and P3_young) are individually labelled.

The English in this document has been checked by at least two professional editors, both native speakers of English. For a certificate, please see:

http://www.textcheck.com/certificate/KzRVfY

The above statement is here to inform reviewers—who may not be native speakers of English—that the English in this document has been professionally checked. If the link to the certificate above is deleted and copied into a letter then the reviewers will not see it.

We STRONGLY recommend that no changes are made. Textcheck should be the last step before final formatting. Typically, authors' changes result in errors in the English, not improvements.

If any text has been misunderstood then please REWRITE the sentence(s) that you need to change, using this file, SAVE, and upload a clean (unmarked) final version of the document to: http://www.textcheck.com/client/submit for a final check. Please do not mark your changes (no highlighting, colored font, bold, etc.) and do not include notes, questions, or comments. Changes that are not because of misunderstanding may incur additional charges; please see: http://www.textcheck.com/text/page/revisions. Requests for a final check should be made within 1 month. For more detailed information, please see: 'When you receive your completed document' at http://www.textcheck.com/text/page/guidelines.

REVISED DOCUMENTS: A previously checked document that needs changed and new sentences checked (such as post review) is termed a 'Revised Document' (http://www.textcheck.com/text/page/fees). Revised Documents should be uploaded via 'Submit Document' in your online account, with a note that the file is a revision of '26092802'. Please do not mark your changes; we will use MS Word to compare the document with the most recent complete previous version in your account. When doing so, we cannot consider extracts or versions earlier than the most recent previous version. It is therefore important to upload complete documents. The fee for a Revised Document is based on the wordcount of ALL new and changed sentences. We do not accept new or revised documents on the basis of requests to 'check only marked text'.

Supplementary Files

This is a list of supplementary files associated with this preprint. Click to download.

- Table12.xlsx